Regenerative Biomaterials, 2016, 1–11
doi: 10.1093/rb/rbv023
Advance Access Publication Date: 29 December 2015
Research Article

OXFORD

Biocompatibility and degradation of tendon-derived scaffolds

Kyle A. Alberti[1] and Qiaobing Xu[1,*]

[1]Department of Biomedical Engineering, Tufts University, 4 Colby Street, Medford, MA 02155, USA

*Correspondence address. Department of Biomedical Engineering, Tufts University, 4 Colby Street, Medford, MA 02155, USA. Tel: +1 617-627-4322; Fax: +1 617-627-3231; E-mail: Qiaobing.Xu@Tufts.edu

Received 20 July 2015; revised 28 October 2015; accepted on 29 October 2015

Abstract

Decellularized extracellular matrix has often been used as a biomaterial for tissue engineering applications. Its function, once implanted can be crucial to determining whether a tissue engineered construct will be successful, both in terms of how the material breaks down, and how the body reacts to the material's presence in the first place. Collagen is one of the primary components of extracellular matrix and has been used for a number of biomedical applications. Scaffolds comprised of highly aligned collagen fibrils can be fabricated directly from decellularized tendon using a slicing, stacking, and rolling technique, to create two- and three-dimensional constructs. Here, the degradation characteristics of the material are evaluated *in vitro*, showing that chemical crosslinking can reduce degradation while maintaining fiber structure. *In vivo*, non-crosslinked and crosslinked samples are implanted, and their biological response and degradation evaluated through histological sectioning, trichrome staining, and immunohistochemical staining for macrophages. Non-crosslinked samples are rapidly degraded and lose fiber morphology while crosslinked samples retain both macroscopic structure as well as fiber orientation. The cellular response of both materials is also investigated. The *in vivo* response demonstrates that the decellularized tendon material is biocompatible, biodegradable and can be crosslinked to maintain surface features for extended periods of time *in vivo*. This study provides material characteristics for the use of decellularized tendon as biomaterial for tissue engineering.

Keywords: biocompatibility, biodegradable, scaffolds, animal

Introduction

Decellularized extracellular matrix (ECM) has been used for a wide variety of applications, including both as a source of biomaterials following processing, and directly as a scaffold for tissue engineering. There are a number of benefits to using decellularized tissue for these applications over synthetic materials including: (i) the presence of biologically active molecules, (ii) the preservation of natural structures with physical cues, (iii) its renewable nature and (iv) overall ultrastructure. The complex biological cues found in the decellularized tissue are representative of the specific source tissue, and can range from biologically active sites found directly on the proteins that predominantly make up the matrix [1], to growth factors and cell adhesion molecules [2,3], acting as a template for future growth.

The behavior of a material in the body following implantation can be crucial to determining whether a tissue engineered construct will be successful, both in terms of how the material breaks down, and how the body reacts to the material's presence in the first place. These two points are one of the reasons why natural polymers are often used for biomedical and tissue engineering applications as they often highly conserved between species, resulting in good biocompatibility and biodegradability.

The biodegradation of a material is important when considering its use. For many tissue engineering applications, the breakdown of the scaffold and regrowth of host tissue is the ideal case, and if possible, the degradation rate of the material will be tuned to match the regrowth [4]. Even more traditional biomedical-oriented applications, such as joint replacement where a non-degradable metallic scaffold is implanted, could be of benefit from a degradable scaffold. For example, a scaffold that promoted bone or cartilage regrowth and provided suitable mechanical properties could prevent the need for revisionary surgeries common to joint replacements [5].

Collagen, which comprises a large amount of many ECM, is typically degraded *in vivo* through proteolytic activity, particularly via MMP-1 (collagenase) activity [6]. The degradation and clearance of implanted ECM materials typically occurs very rapidly following implantation [7], thus many collagen-based biomaterials are crosslinked prior to use. Crosslinking has been shown to reduce the degradation of collagen [8,9], as well as to reduce any potential immune response that the collagen may elicit through masking of potential antigenic markers [10].

We have developed a sectioning-based fabrication technique, called Bioskiving, which allows fabrication of two- and three-dimensional scaffolds directly from decellularized tendon sections using sectioning, stacking and rolling [11]. This process maintains the highly aligned hierarchical structure of the native collagen found in tendon which provide nanotopographical growth guidance cues [12,13], and improves the mechanical properties [14]. Scaffolds created using this process could find use in many tissue engineering, and biomedical applications where the biocompatibility of the material and degradation characteristics would be important considerations for use. Here, the degradation characteristics of the material, in a non-crosslinked and crosslinked state, are investigated both *in vitro*, and *in vivo*, along with the biocompatibility and response to subcutaneous implantation.

Methods and materials

Scaffold fabrication

Tendon sections were fabricated as previously described [11,14]. Briefly, 20 mm × 20 mm × 2 mm tendon sections, from Bovine Achilles tendon, were decellularized at 4 °C using a 1% sodium dodecyl sulfate solution with 1 mM Tris–HCl and 0.1 mM EDTA, for 48 h with the decellularization solution being changed after 24 h. Following this, the samples were rinsed for 24 h with deionized water (diH_2O), and frozen at − 20 °C. The samples were then cut into 50 μm thick sections using a cryostat microtome. The frozen sections were placed on room temperature polytetrafluoroethylene blocks, in stacks of 10, with fiber orientations alternating by 90° in adjacent sections. These stacks were then allowed to dry, rinsed with diH_2O three times, and then dried again. The samples were then used in this state as non-crosslinked (NC) or crosslinked in a glutaraldehyde (GA) solution in phosphate buffered saline (pH 7.4). For *in vitro* degradation testing, the samples were crosslinked in GA at concentrations of 0.625% and 2.5% for 20 min and 2.5% for 1 h, and in 2.5% for 1 h for *in vivo* degradation testing. Poly(lactic-*co*-glycolide) (75:25, MW:76 000–115 000) (PLGA) samples were also fabricated for *in vivo* testing by dissolving PLGA in acetone at 100 mg/ml on a shaker overnight. Once dissolved it was cast in a glass petri dish and placed into a fume hood for 3 days to evaporate. It was then placed into a vacuum oven at room temperature overnight to remove any residual solvent; the resulting film was 0.2 mm thick. The PLGA was then rinsed 3 times in diH_2O and allowed to dry.

For *in vitro* testing, the samples were then dried overnight in a vacuum desiccator and cut into equal rectangular strips weighing 10–12 mg and roughly 20 × 5 mm in size. For *in vivo* testing, each of the larger samples (NC, GA, PLGA) was then cut into 5 × 5 mm squares and immersed in ethanol for 1 h followed by 1 h under the UV light in a tissue culture hood to sterilize them. The samples were then placed into autoclaved glass vials until implantation.

Collagenase degradation

Dried samples were accurately weighed and the weights recorded. Each sample was placed into a 24 well plate and 0.5 ml 0.1 M Tris–HCl with 0.005M $CaCl_2$ (pH 7.4) added to hydrate the samples for 20 min. To this 0.5 ml of a collagenase solutions containing 2 mg/ml collagenase (Clostridium histolyticum (125CDU/mg), Sigma) in the same Tris–HCl buffer. This resulted in a final concentration of 1 mg/ml collagenase or roughly 10–12 CDU/mg of sample. These plates were placed into a humidified incubator at 37 °C and 5% CO_2 on a shaker at 80 rpm. The samples were digested for 8, 24, 48 or 96 h before being removed from the incubator, rinsed 3 times in diH_2O and dried for 24 h in a vacuum desiccator. The samples were then reweighed and percent mass remaining calculated.

Mechanical testing

Samples from each degradation condition ($n = 4$) were rehydrated in PBS and tested under uniaxial tension at a rate of 5%/min on a mechanical testing apparatus (Instron, Norwood, MA) with a 1000 N load cell until failure. Ultimate tensile strength (UTS) was calculated from the load vs extension data based on initial sample geometries. UTS was determined as the maximum stress of each sample's stress-strain curve.

SEM analysis

For scanning electron microscope (SEM) analysis of samples test *in vitro*, a small piece was trimmed from the end of each tendon sample prior to mechanical testing. For SEM analysis of samples tested *in vivo*, the implant was removed from the other half of the excised tissue sample that had not been sectioned, using forceps and blunt dissection. For samples that were highly integrated with the surrounding tissue, care was taken to avoid disrupting the structure as much as possible. The samples were dehydrated using graded ethanol followed by hexamethyldisilizane (HMDS). The samples were then placed on stub mounts and sputter coated with 3 nm Pt:Pd 80:20 using a Cressington 208HR Sputter-coater (Cressington Scientific, Watford, Hertfordshire, UK) to a thickness of 3 nm and imaged using a Zeiss Ultra-55 Scanning Electron Microscope (Zeiss, Oberkochen, Germany). Representative images of the surface were taken.

Subcutaneous implantation

The research protocol was approved and in compliance with Tufts University's Institutional Animal Care and Use Committee (IACUC, protocol # M2013-58) in accordance with the Office of Laboratory Animal Welfare (OLAW) at the National Institutes of Health (NIH). Two samples were implanted into the back above the left and right hind flank of male Sprague–Dawley rats. The implantation procedure was as follows: each animal was weighed and anesthetized via 2–3% isoflurane inhalation and appropriate analgesics provided. The surgical area was shaved and cleaned and a surgical drape is placed onto the animal with a hole cut to expose the surgery site. Two, 1 cm incisions were made through the skin on the upper back above the right and left hind legs. One implant was placed into each wound site and the skin closed with 4-0 vicryl sutures in a running subcuticular manner. The animals were allowed to recover and wound healing monitored daily until completely healed. There were no complications with any of the surgeries.

At 1, 3 or 9 weeks the animals were sacrificed and the implant and surrounding tissue was excised, noting tissue condition and any

inflammation. The samples were placed into freshly prepared 4% paraformaldehyde (pH 7.4) for 1 h, and then rinsed in PBS.

Histology

Excised samples and surrounding tissue were placed in a 30% sucrose solution for 2 days. They were then cut in half and one half placed in optimal cutting temperature (OCT) compound for 1 h at room temperature. These blocks were then snap frozen on dry ice and stored at −20 °C until sectioning. The blocks were sectioned at 6 μm thick and the sections placed on Superfrost Plus slides. The slides were dried at room temperature overnight and then frozen until staining. The sections were stained with hematoxylin and eosin (H&E) using standard techniques, or Masson's trichrome stain using the manufacturer's protocol (HT15, Sigma). The slides were then mounted with DPX mounting media (Sigma) and cover slipped. Images of the sections were taken with 4× and 40× objectives using a Keyence BZX fluorescence microscope.

For immunohistochemical staining samples were allowed to come to room temperature and rinsed 3 times using PBS, and blocked for 1 h at room temperature using 10% goat serum in PBS. The slides were then rinsed 3 times using PBS with 0.1% Tween-20 (PBST), decanted, and a primary antibody (mouse anti-CD68, Pierce MA5-13324) diluted 1:200 in 1% bovine serum albumin in PBST, applied. The samples were incubated for 2 h at room temperature, covered from light in a humidified chamber, after which they were rinsed 3 times with PBST. Endogenous peroxidase activity was neutralized using freshly prepared 0.3% H_2O_2 in PBS for 15 min. This was decanted and the samples rinsed again, and the secondary antibody (horse radish peroxidase-conjugated goat anti-mouse (F_{AB}) adsorbed against human and rat serum, Sigma A3682) diluted 1:200 in 1% BSA in PBST, applied for 1 h at room temperature. The slides were then rinsed 3 times in PBST and SigmaFAST DAB with metal enhancer used to develop the peroxidase for 15 min. Following this, the sections were counterstained with Gills Hematoxylin for 10 min, blued in acid alcohol, followed by Scott's tap water substitute, dehydrated using graded ethanol, followed by xylene, and mounted.

Sample quantification

Tissue capsule thickness was measure by imaging four random locations around the outside of the implant at 400×. The capsule was defined as the area between the implant and the surrounding material until it returned to normal ECM structure appearance. At each of these locations, four measurements were taken using ImageJ. The average capsule thickness was calculated for each of the sections and implants.

Total cell number was measured from H&E stained samples (Supplementary Fig. S1), by counting the total number of cells in a 250 × 250 μm area extending out from the implant. The total number of cells was measured at four locations per sample and averages calculated for each implant and implant material.

Statistics

All values reported as mean ± standard error and a sample size of $n = 4$ was used for all conditions. Differences in UTS and modulus were analyzed by analysis of variance (ANOVA) with *post hoc* Tukey's testing using IBM SPSS software (IBM, Armonk, NY). While differences in capsule thickness and cell number were analyzed for statistical significance by performing a two-way Student's t-test assuming an equal variance with an α-value of 0.05. A *P*-value of <0.05 was determined to be statistically significant.

Results

Collagenase degradation

Samples (NC or GA-crosslinked 0.625% GA for 20 min, 2.5% GA for 20 min, 2.5% GA for 1 h), were degraded in a collagenase solution for 8, 24, 48 or 96 h. The samples were then dried overnight and weighed, and the percent mass loss calculated (Fig. 1A). Highly crosslinked samples (2.5% GA for 1 h) lost 1.9% after 96 h, moderately crosslinked samples (2.5% GA for 20 min) lost 2.1%, and low crosslinked (0.625% GA for 20 min) samples lost 4.3% of their initial weight, while non-crosslinked samples lost 33.5% of their initial weight.

Degradation mechanical properties

Following degradation, the tendon sections were rehydrated in PBS and ultimate tensile strength of the material measured using uniaxial tensile testing (Fig. 1B). Highly crosslinked samples had an initial UTS of 4.71 ± 0.29 MPa which decreased to 2.45 ± 0.45 MPa after 96 h (48.0% loss). Moderately crosslinked samples had an initial UTS of 3.75 ± 1.36 which decreased to 1.79 ± 0.12 MPa after 96 h (52.32% loss). Lightly crosslinked samples had an initial UTS of 2.28 ± 0.26 MPa which decreased to 0.26 ± 0.07 MPa after 96 h (88.5% loss). NC samples had an initial UTS of 0.30 ± 0.02 MPa which decreased to 0.03 ± 0.8 MPa after 96 h (88.4% loss).

Fiber morphology

Following degradation NC and GA samples were imaged using SEM for surface fiber morphology (Fig. 2). Fiber structure can clearly be seen in the non-crosslinked samples, and the crosslinked

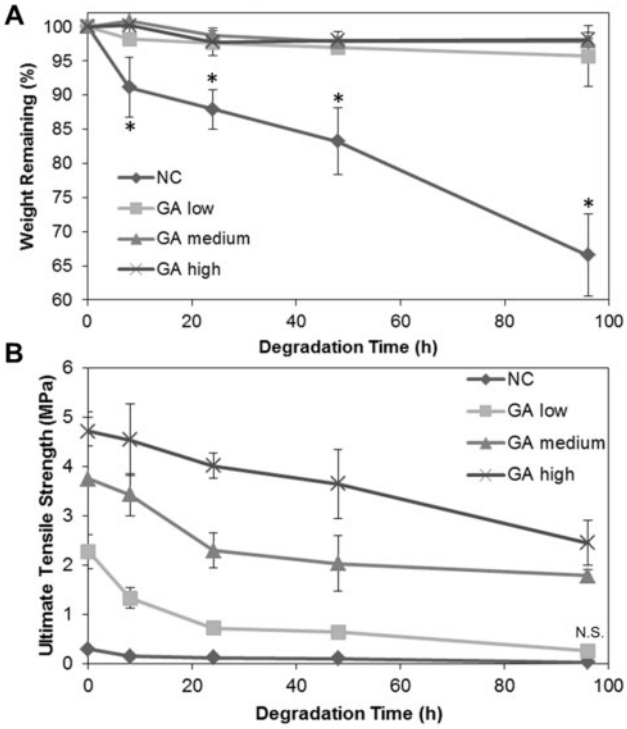

Figure 1. (A) Mass remaining in bioskiving scaffolds following bacterial collagenase degradation. ($n = 4$) * = P values < 0.05. (B) ultimate tensile strength of bioskiving scaffolds following bacterial collagenase degradation. ($n = 4$) all values statistically significant (P values < 0.05) except GA low vs NC at 96 h indicated N.S.

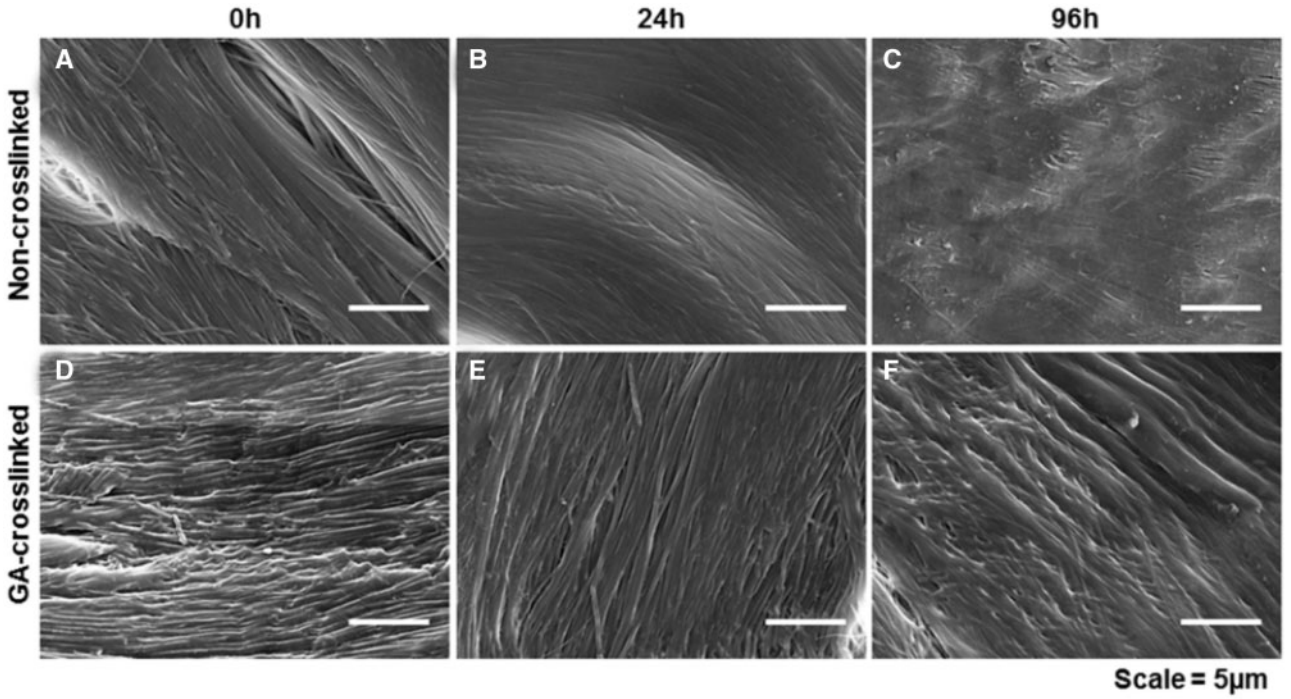

Figure 2. Scanning electron micrographs of: (A) non-crosslinked samples prior to collagenase degradation, (B) after 24 h, (C) after 96 h and (D) GA-crosslinked samples prior to degradation, (E) after 24 h, (F) after 96 h.

samples (2.5% GA for 1 h). After 24 h, most of the surface structure in the non-crosslinked samples is gone while after 96 h, the surface is largely flat with little to no definition. The GA-crosslinked samples however retain well-defined fiber structures for 24 h, along with some fiber structure after 96 h. The fibers in the GA-crosslinked samples after 96 h have been degraded to some degree, appearing similar to the fibers in the non-crosslinked 24 h samples. Some peaks and valleys between fiber bundles are still observable, as are more macroscopic aligned topographies.

In vivo subcutaneous implantation

To assess the biological response to tendon-derived collagen sections, non-crosslinked, GA-crosslinked, and PLGA control samples were implanted subcutaneously into the back of male Sprague–Dawley rats following ASTM Designation: F1408 – 97. Samples were implanted for 1, 3 or 9 weeks, with 6 samples per condition, per time point. At the time of sacrifice, the condition of the implant and surrounding tissue was noted, and both the implant and tissue excised together.

Figure 3 shows representative images of the explanted tissues. One week following implantation, a well-defined edge on the samples can be observed. No significant local redness indicating inflammation was observed, however the vasculature surrounding the implant did appear to be dilated. Again at week 3, no local tissue redness appears and the surrounding vasculature appears to have largely subsided. The edges of the implants are beginning to round over, possibly either from degradation or integration into the surrounding tissue. By week 9, significant degradation had occurred in the non-crosslinked and PLGA samples. Three out of six non-crosslinked implants were no longer observable, and those that remained appeared to have little integrity remaining. Four of six PLGA samples had formed into a round shape. Little change was observed in the GA-crosslinked sample between weeks 1, 3 and 9.

Histological evaluation

Histological evaluation of the implants at each time point (Low magnification—Fig. 4, High magnification—Fig. 5) shows similar results. At week 1, the non-crosslinked samples have swollen from their initial dry thickness (200 μm) to 600–700 μm (Fig. 4A). There is also a large number of cells directly surrounding the material along with some loosely packed collagenous tissue. Small neovasculature can be seen developing around the perimeter of the implant.

By week 3, the cellular response has dramatically changed. The tendon sample has been inundated with a large number of cells (Fig. 4B). There are fewer cells surrounding the tissue but many more in the sample that have grown in between the fibers of the individual sheets and cells can be seen growing or moving along the collagen fibers that are running in the plane of the image, indicating that these cells are likely still being influenced and oriented by the nanotopography (Fig. 5B). Additionally, larger more developed vasculature can be seen growing near the implant. Individual sheets have largely been degraded, but some change in fiber orientation can still be observed between adjacent sections and the collagenous network surrounding the cellular infiltration is largely dispersed. At week 9, the majority of the non-crosslinked samples are no longer clearly visible in the histological images (Fig. 4C). The samples that had been visible at explant in Fig. 3 had some dense areas of collagen present in the hypodermis; however, surprisingly in these areas there is no longer a large cellular response.

The GA-crosslinked samples at week 1 underwent little hydration, resulting in minimal separation between collagen fibers and sheets, and reduced cell infiltration (Fig. 4D). The thickness of the cell layer surrounding the GA sample was greater and denser, and a

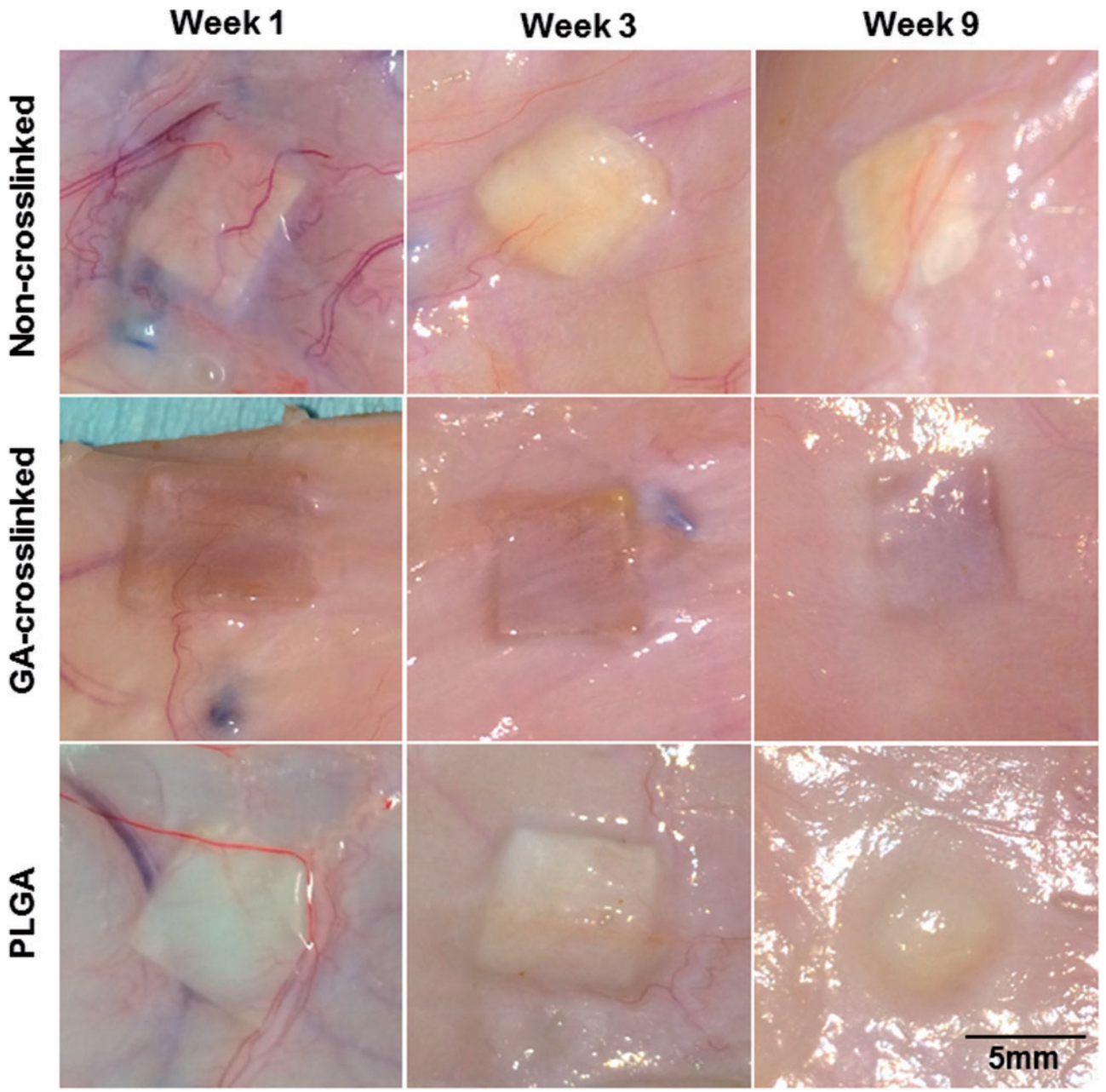

Figure 3. Representative photographs of subcutaneously implanted samples (non-crosslinked tendon, GA-crosslinked tendon and PLGA) after 1, 3 or 9 weeks of implantation. Note: not all week 9 non-crosslinked samples were visible. 5 mm scale bar relevant for all images.

well-defined layer 1–2 cells thick directly surrounding the implant (Fig. 5D), which was absent in the non-crosslinked samples. At week 3, a large cellular response is also seen around the GA-crosslinked samples, along with some vascular development nearby (Fig. 5E). However, the cells here are largely confined to the perimeter of the sample, and are unable to penetrate in between the individual sections, or within the fibers of the collagen. By week 9, the immediate area surrounding the implant remains highly cellular (Fig. 4F), and it appears that cells begin to penetrate between sheets of the construct (Fig. 5F).

PLGA samples were used as known biocompatible and biodegradable control. At week 1, the PLGA samples had a dense cellular layer around it (Fig. 4G) and a 1–2 cell thick layer (Fig. 5G) similar to the GA-crosslinked samples. At week 3, an increase can be seen in cell density; however no cell infiltration is seen. At week 9 the cellularity is decreased and confined to directly around the implant. Vasculature can also be seen at all time points following explant.

Histological quantification

As a quantitative assessment of these results the thickness of the inflammatory capsule surrounding each implant was measured. The inflammatory capsule was defined as the area between the implant and the area that returns to normal, extracellular matrix, and contains granulation tissue primarily comprised of blood vessels, fibroblasts and immune cells. Figure 6A shows the thickness of each capsule. Initially there was a high degree of cell growth and encapsulation at week 1 for all samples. Over time the degree of

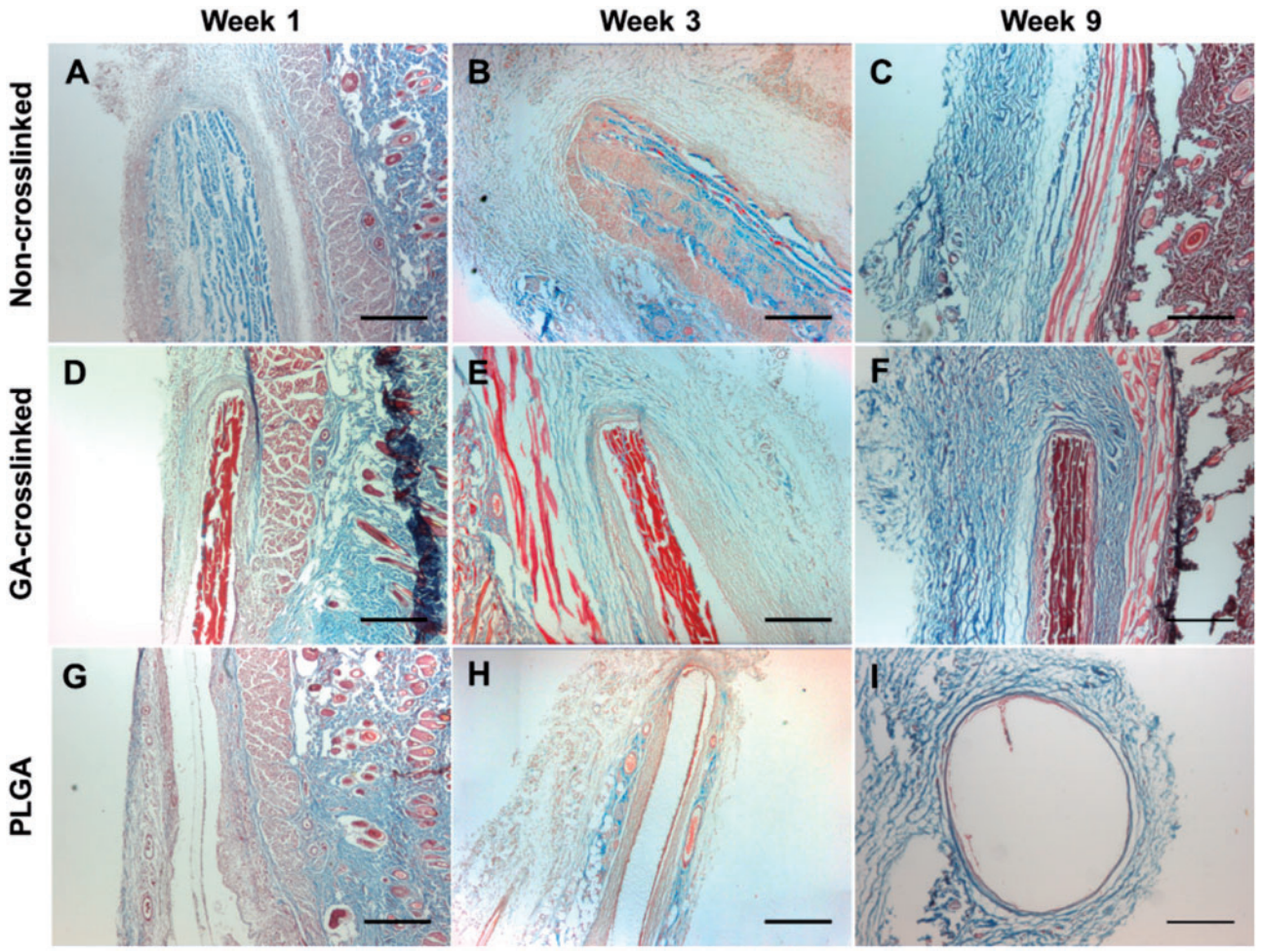

Figure 4. Low magnification images of masson's trichrome stained sections of implanted: non-crosslinked decellularized tendon sections (A–C), GA-crosslinked decellularized tendon sections (D–F) and PLGA (G–I). Scale bars are 500 μm.

encapsulation decreased for all samples, disappearing for the non-crosslinked samples as they were nearly completely degraded.

The number of cells surrounding each implant (Fig. 6B) was also quantified to elucidate the biological response. Four random locations around each implant were imaged on H&E stained sections, and the number of cells in the area from the implant to the edge of one field of view at 400x magnification (350 μm) counted. Analysis of cell number correlates with the phenomena described in the histological images.

Initially there are a large number of cells surrounding the non-crosslinked implant. This number then decreases as the cells infiltrate the scaffold, and finally decreases further as the samples near complete degradation. A similar trend is seen with the GA-crosslinked samples; however, the decline in cell number is not as precipitous as the implant is not completely degraded but the inflammatory response has decreased by this point

Immunohistochemical analysis

Immunohistochemical staining for macrophage cells (Supplementary Fig. S2) was quantified as total number of $CD68^+$ cells in a given high powered field (HPF) (Fig. 7). Initially there are a high number of $CD68^+$ cells in the GA and PLGA samples; however, this decreased at both 3 and 9 weeks. The non-crosslinked sample initially had fewer $CD68^+$ cells however at 3 weeks the number of positive cells increased, followed by a decrease to levels similar to GA and PLGA samples at week 9. If these values are normalized to a percent of the total cells in the same given HPF, there is little difference in each of the time points between NC, GA and PLGA samples (Supplementary Fig. S3).

Sample morphology

In the *in vivo* degraded non-crosslinked samples (Fig. 8) a high degree of alignment in the collagen fibers prior to implantation can be observed, while at week 1 many of the fibers are disrupted, but still identifiable, with some areas containing disarrayed collagen fibrils. At week 3 little to no fiber architecture can be seen and the entire surface appears to be a tangled network of fibers. Following week 9, the samples that were able to be identified and separated, displayed no fiber structure or alignment or fibril structure. At week 9 however, bundles of collagen fibers containing aligned fibrils can be seen again, however the overall fiber architecture is disorganized and a likely a result of resorption and redeposition of host collagen.

In contrast, highly aligned collagen fibers and fibrils can be seen prior to implantation and at weeks 1 and 3 within the GA-crosslinked sample. At week 9, some of the fiber morphology is lost but a large number of collagen fibers are still identifiable. The PLGA samples show development of pores in the surface at week 1 and 3 and large surface degradation by week 9.

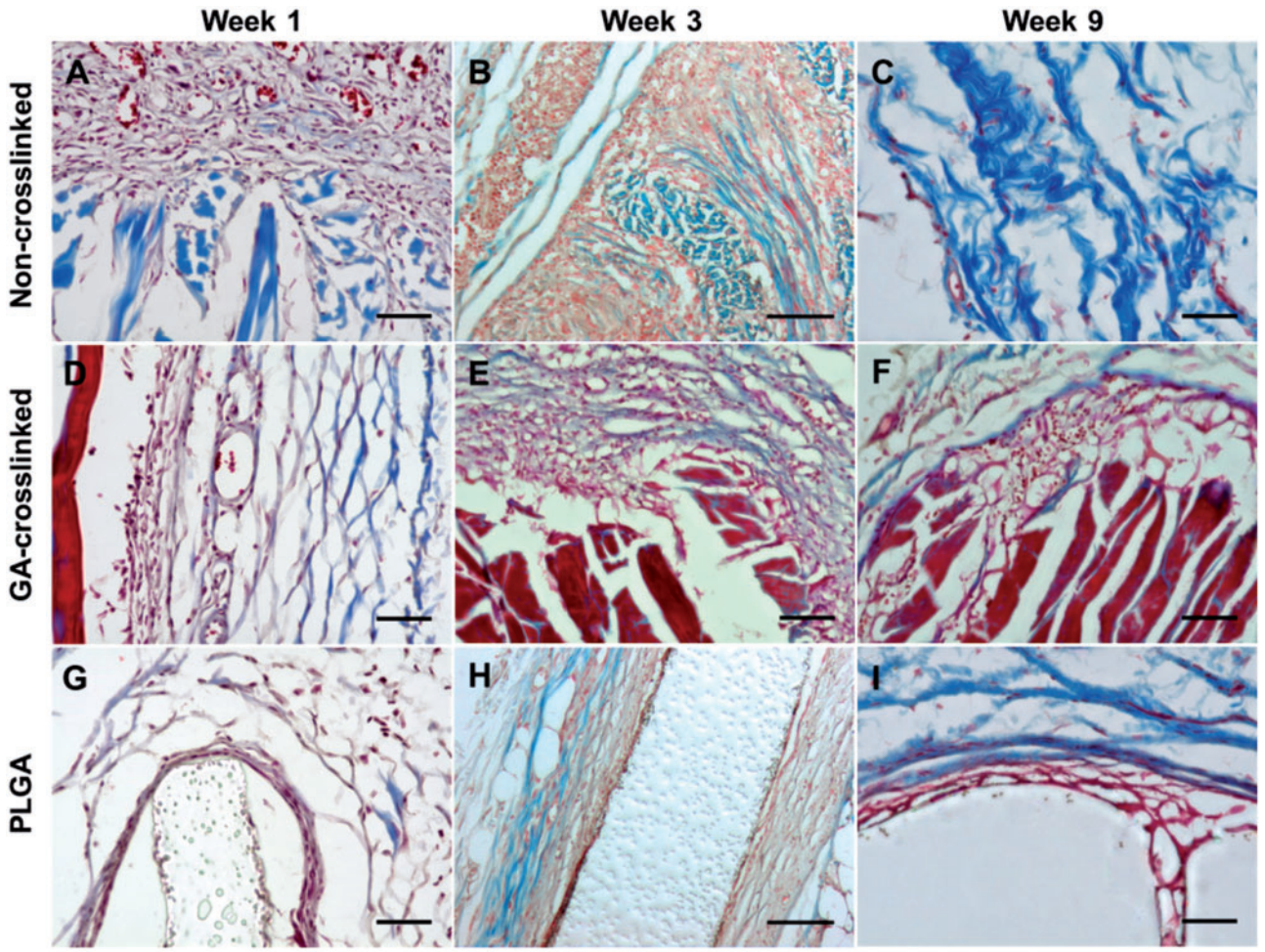

Figure 5. High magnification images of masson's trichrome stained sections of implanted: non-crosslinked decellularized tendon sections (A–C), GA-crosslinked decellularized tendon sections (D–F) and PLGA (G–I). All scale bars are 50 μm.

Discussion

Prevention of premature degradation is important for the tendon-derived scaffolds as one of the major features of the fabrication technique is maintenance of the highly aligned collagen fibrils and fibers which have the potential to guide cellular growth. If degradation were to occur too rapidly, prior to adequate cell growth and infiltration, these structures would not be able to provide their nanotopographical growth guidance cues.

Due to these concerns, the degradation characteristics of the tendon-derived material were assayed. An initial analysis into the degradation rate was conducted on decellularized tendon sections after various degrees of crosslinking, via degradation with bacterial collagenase. One concern regarding bacterial collagenase is that *Clostridium histolyticum* collagenase has been shown to cleave collagen into several small fragments [15], whereas mammalian collagenase cleaves it into only two [16]. However, degradation *in vitro* using bacterial collagenase has been shown to correlate well with *in vivo* degradation, despite the differences in the cleavage mechanism [17]. Therefore, *in vitro* analysis can be used as a preliminary mechanism for determining degradative behavior [18].

As expected, glutaraldehyde reduces the degradability of the collagen sections. Variations in the crosslinking density and type of crosslinker used also have an impact on how much weight is lost per sample, with highly crosslinked (1.9%), moderately crosslinking (2.1%), lightly crosslinked samples losing (4.3%) substantial less mass, compared to non-crosslinked samples (33.5%) (Fig. 1A). The difference in the changes in weight of the crosslinked sample were not as dramatic as anticipated however, and may be a result of the collagenase cleaving the collagen fibers, however the fragments that have been cleaved remain attached to the bulk via interfibrillar GA crosslinks.

This would not affect the weight; however, it could have a substantial impact on the mechanical properties. Mechanical analysis showed this to be a likely scenario as the ultimate tensile strength of GA-crosslinked samples was significantly reduced following extended periods of collagenase degradation (Fig. 1B). The ultimate tensile strength of maximally crosslinked GA scaffolds reduced by nearly half of the initial value following 96 h of degradation, whereas the already low mechanical properties of the non-crosslinked samples reduced further, and much more rapidly. Interestingly, a significant difference in initial and final tensile strength was observed for all GA-crosslinked samples despite only a

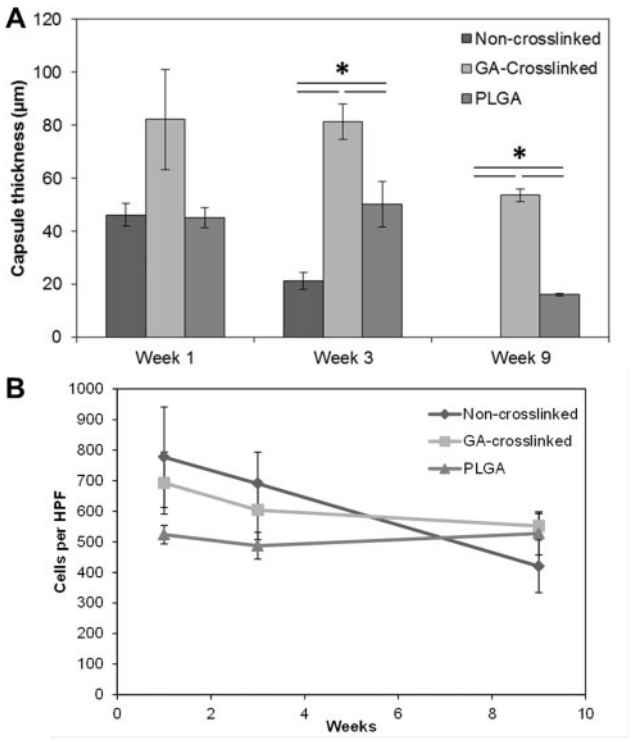

Figure 6. (A) Inflammatory capsule thickness of non-crosslinked, GA-crosslinked and PLGA samples at 1, 3 and 9 weeks post implantation. * = $P < 0.05$. (B) average cells per high powered field (HPF) (400×) extending from the edge of the implant out 0–350 μm away. No statistical difference was observed between samples at 1 week, 3 weeks or 9 weeks.

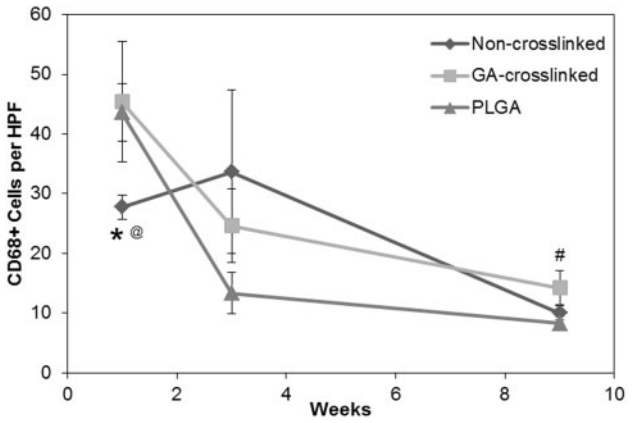

Figure 7. Quantification of total number of $CD68^+$ cells present per high powered field (HPF) surrounding each of the implant conditions: Non-crosslinked, glutaraldehyde-crosslinked and PLGA, after 1, 3 and 9 weeks of subcutaneous implantation. * indicates P values < 0.05 for NC vs GA, @ indicates P values < 0.05 for NC vs PLGA, # indicates P values < 0.05 for GA vs PLGA.

minimal change in sample weight. Maintenance of mechanical properties following degradation would be an important factor to consider, specifically for load-bearing applications like tendon or ligament repair.

One concern regarding the use of collagenase here *in vitro* is that the collagenase in solution was not replenished during the degradation experiments, which may have led to reduced activity over time; however, the continued degradation of the non-crosslinked sample, along with the reduction in mechanical strength of all samples, indicates that some enzymatic activity remained.

As growth guidance cues are an important aspect of this material, maintenance of fiber morphology will be important to consider. SEM analysis of samples can indicate the status of the fibers following collagenase degradation. Figure 2 shows the morphology of samples prior to degradation, and after 24 and 96 h of degradation. The rapid loss of the collagen fiber structure in the non-crosslinked samples compared to the GA-crosslinked samples verifies the results of the previous experiments. All three experiments indicate that a scaffold designed to influence cell growth for prolonged periods of time may require some degree of crosslinking to retain this ability. The results presented here indicate that loss of fiber structure occurs rapidly; however, *in vivo* it is likely that numerous cells will interact with these features prior to their degradation. These cells themselves may become aligned, which could further act as a template for cell alignment, providing topographical cues beyond the life of the scaffold. For example, this type of secondary alignment guidance has been demonstrated with neurons following morphologies based on a Schwann cell template [19].

In vitro analysis can only go so far towards evaluating a materials performance, and *in vivo* implantation is often necessary, and subcutaneous implantation is often used to assess biocompatibility. The initial macroscopic observation (Fig. 3) of the NC, GA and PLGA samples further confirms that GA crosslinking reduces the degradability of the tendon-derived material. The additional fact that several NC samples degraded while others had not completely degraded by week 9 may also point to the fact that there may be slight differences in either the animal, implantation procedure, or in sample handling in processing. Other physiological responses that were common between all samples, such as vascular dilation are likely associated with the acute and chronic inflammatory phase that occurs 1–2 weeks following implantation [20]. Similarly, the fact that four of six PLGA samples had been compressed into a round shape, likely a result of myofibroblast contracture [21,22], suggests that these variations are normal.

Histological investigation further elucidates the difference in cellular response between the NC and GA samples (Figs 4 and 5). At week 1, NC samples have swelled from their initial size, due to hydration, which is also observed when they are hydrated ex vivo. This hydration may have further allowed cell infiltration into and between the ends of the layers and between the outermost layers, which was not observed with crosslinked samples that did not swell. At week 3 the differences in cellular response between the implants becomes more apparent. The NC tendon sample has been inundated with a large number of cells, combined with additional tissue deposition, likely granulation tissue containing host fibroblasts and macrophages as part of an inflammatory response. This is further confirmed with $CD68^+$ staining to indicate cells of a macrophage lineage where larger cells are observable. Traditionally a large macrophage response is viewed as detrimental, and associated with chronic inflammation; however, it has also been shown to be crucial to promoting a constructive remodeling response, particularly with ECM scaffolds [23], and may be dependent on M1 vs M2 macrophage phenotype.

As a result of this large cellular infiltration, the NC samples are largely degraded by week 9, and those that remained dense areas of collagen that lacked a large cellular response. It is possible that in these cases, the tendon sections were completely degraded and in the process, new collagen put down using the tendon as a template,

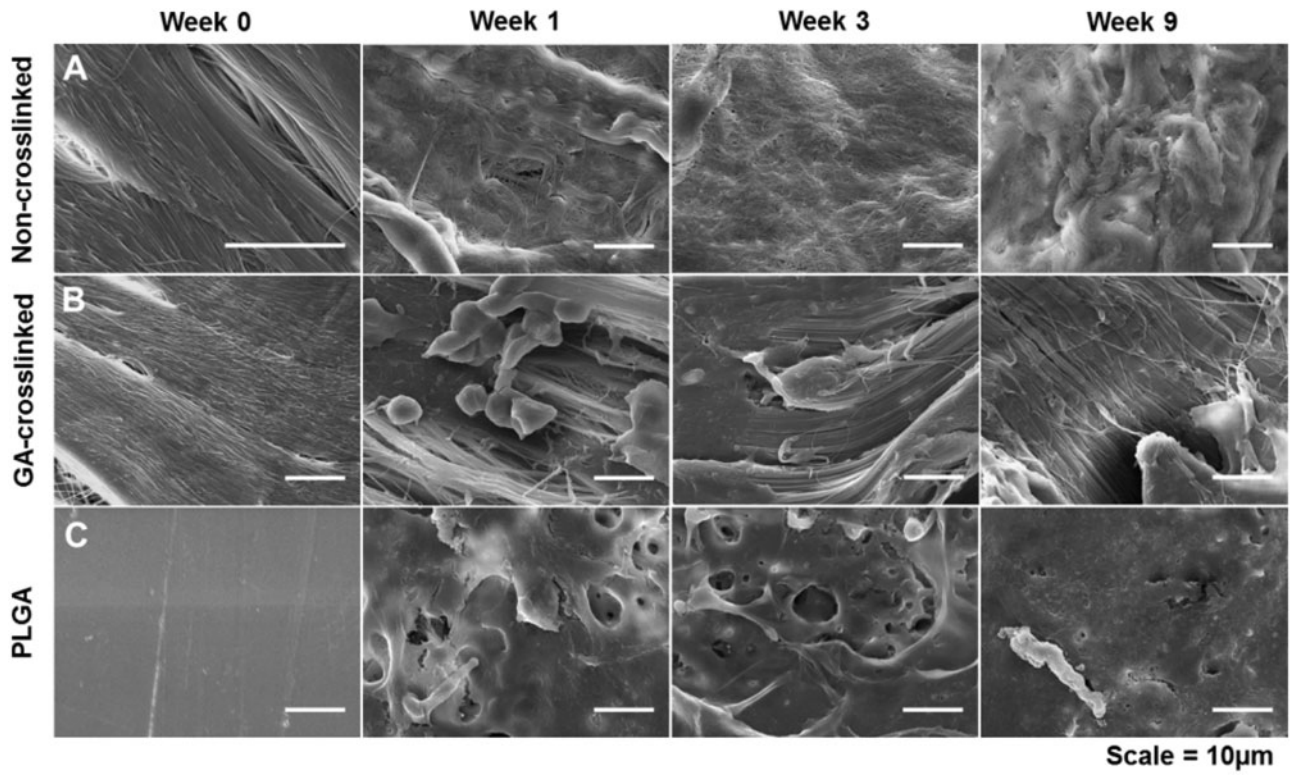

Figure 8. Electron micrographs of the surface of implants prior to implantation and at weeks 1, 3 and 9 following excision of (A) non-crosslinked, (B) GA-crosslinked and (C) PLGA.

resulting in the visible structures—Oliver *et al.* observed a 60% degradation of collagen scaffolds within 20 weeks of implantation, accompanied by a an equal amount of collagen regeneration, using ^{3}H-labelled collagen samples [24].

In contrast, the GA samples had less cell infiltration, but a layer of cells directly around it. This lack of cell infiltration may be desirable for applications like nerve guidance conduits where you would not want fibroblast infiltration into the lumen of the conduit. Interestingly, the GA-crosslinked sections stain red, rather than blue as is expected with a Masson's trichrome stain. This is likely due to the large increase in density of the fibrils due to the crosslinking, as Analine Blue and Biebrich scarlet-acid fuchsin, used in Masson's trichrome staining, rely on differential penetration into tissue based on the molecule size. A return to expected staining color was observed in the edges of several sections with a high degree of cellular infiltration, where areas in immediate contact with cells stain blue as collagen is expected to. This is likely a result of the degradation of the material by the cells, which in effect reduces the density and allows for typical staining.

Also of note, is that the GA-crosslinked samples did not present with any overt signs of toxicity or necrosis to the surrounding tissue; however, the potential of cytotoxicity must be considered when using GA. The high level of cellularity surrounding the implant at week 3 may indicate that the GA breakdown byproducts are not too detrimental as to prohibit cell growth in in immediate area; however they may have an effect on the cell type which remains to be analyzed. These data indicate that the non-crosslinked tendon samples are biocompatible and biodegradable, as they undergo integration followed by resorption. The GA-crosslinked samples elicit a similar response to PLGA. These implants appear to elicit some degree of a foreign body response. Primary evidence of this is the one- to two-cell layer that surrounds the latter samples, indicating a foreign body reaction [25].

Overall, a comparison between the three conditions indicates that the non-crosslinked collagen is very well accepted by the body and rapidly degraded. There appears to be an inflammatory response, likely M2 macrophages associated with constructive remodeling, rather than rejection; a similar phenomenon is seen with decellularized dermis and small intestine [26,27]. Cells quickly infiltrate and degrade the material, and if in direct contact with the tendon may be guided by the material for at least 3 weeks. By week 9, the non-crosslinked sample has been degraded to the point where it is difficult to identify histologically, and no longer elicits a cellular response. At this point, the material would provide little to no mechanical strength or nanotopographical guidance cues. The GA-crosslinked implant and the PLGA implant appear to elicit similar reactions characterized by inflammation with dense cellular tissue at weeks 1 and 3, neither of which penetrates significantly into the material. At week 9, the cellular response and inflammation have largely subsided and are isolated to the area directly surrounding the implant, as the materials enter a state of biological tolerance following the inflammatory response.

These results are consistent with previous reports of acellular dermal scaffolds exhibiting a lack of long term inflammation when implanted subcutaneously; and GA crosslinked scaffolds exhibiting a slight response [28–31]. The reported amount of degradation in decellularized ECM scaffolds also varies greatly, with complete degradation occurring in scaffolds without crosslinking in 50 days and 0–15% degradation in glutaraldehyde crosslinked [24,31], some absorption after 20 weeks for Permacol scaffolds [32], and 28 days for Alloderm [33].

Quantification of these observed histological occurrences confirms the qualitative assessment. With many implants you would expect the capsule thickness to increase over time and change composition as the granulation tissue is replaced with fibrotic tissue (collagen), particularly for non-biodegradable samples, as the body attempts to wall off the implant. That is not observed here as the inflammatory capsule appears to resolve itself over time. This is most likely due to the xenogeneic collagen eliciting some immune response that then abates as acute and chronic inflammatory responses subside. This phenomenon has been observed previously with xenogeneic collagen, including bovine dermal collagen [34,35]. Quantification of macrophage presence appears to indicate similar, all sample types elicit some degree of macrophage response which may be involved in host remodeling or chronic inflammation depending on sample type, but this must be further investigated.

Again as discussed regarding the *in vitro* degradation, one of the anticipated applications for this material is the guidance of cellular growth, the degradation of the material would clearly impact its potential to achieve this. A similar trend is observed *in vivo*, where fiber orientation and morphology in NC samples is quickly disrupted and degraded which would negatively impact the material's ability to orient cellular growth. GA crosslinking prevents this degradation and retains fiber structure.

Conclusion

This work demonstrates the biological properties of the tendon-derived material and gives insight into the potential biological responses and the ability to predict the behavior in different applications. One consideration in evaluating the material is that applications may require a specific degradation rate to correspond to variations in tissue regeneration and host response. *In vitro* degradation experiments here show the rate can be tuned through crosslinking, extending the lifetime of the material mass, mechanical strength, and the underlying collagen fiber morphology.

The *in vivo* response of the material demonstrates that the decellularized tendon material is biocompatible, biodegradable and can be crosslinked to maintain surface features for extended periods of time *in vivo*. Non-crosslinked samples rapidly degrade following a large macrophage response, while glutaraldehyde-crosslinked and PLGA samples elicit a similar mild foreign body reaction; however, these issues abate long term. The *in vivo* results also confirm that collagen fiber morphology is quickly disrupted when the samples are not crosslinked and that the morphology can be maintained following crosslinking.

Acknowledgements

We would like to thank Caleb Neufeld for proof reading of the manuscript. Q.X. acknowledges Pew Scholar for Biomedical Sciences program from Pew Charitable Trusts and NIH (1R03EB017402-01). K.A. acknowledges the IGERT fellowship from NSF and a Predoctoral Fellowship from the American Heart Association. This work utilized the facilities at the Harvard University Center for Nanoscale Systems (CNS), a member of the National Nanotechnology Infrastructure Network (NNIN), which is supported by the National Science Foundation under NSF award no. ECS-0335765.

Supplementary data

Supplementary data are available at *REGBIO* online.

Conflict of interest statement. None declared.

References

1. Kleinman HK, Philp D, Hoffman MP. Role of the extracellular matrix in morphogenesis. *Curr Opin Biotechnol* 2003; **14**:526–32.
2. Hoganson DM, O'Doherty EM, Owens GE *et al*. The retention of extracellular matrix proteins and angiogenic and mitogenic cytokines in a decellularized porcine dermis. *Biomaterials* 2010; **31**:6730–7.
3. Ning L-J, Zhang Y, Chen X-H *et al*. Preparation and characterization of decellularized tendon slices for tendon tissue engineering. *J Biomed Mater Res a* 2012; **100**:1448–56.
4. Vepari C, Kaplan DL. Silk as a Biomaterial. *Prog Polym Sci* 2007; **32**:991–1007.
5. Pabinger C, Berghold a, Boehler N *et al*. Revision rates after knee replacement: Cumulative results from worldwide clinical studies versus joint registers. *Osteoarthr Cartil* 2013; **21**:263–8.
6. Woessner JF. Matrix metalloproteinases and their inhibitors in connective tissue remodeling. *Faseb J* 1991; **5**:2145–54.
7. Record RD, Hillegonds D, Simmons C *et al*. in vivo degradation of 14C-labeled small intestinal submucosa (SIS) when used for urinary bladder repair. *Biomaterials* 2001; **22**:2653–9.
8. Harriger MD, Supp aP, Warden GD *et al*. Glutaraldehyde crosslinking of collagen substrates inhibits degradation in skin substitutes grafted to athymic mice. *J Biomed Mater Res* 1997; **35**:137–45.
9. Olde Damink LH, Dijkstra PJ, van Luyn MJ *et al*. In vitro degradation of dermal sheep collagen cross-linked using a water-soluble carbodiimide. *Biomaterials* 1996; **17**:679–84.
10. Badylak SF, Gilbert TW. Immune response to biologic scaffold materials. *Semin Immunol* 2008; **20**:109–16.
11. Alberti KA, Xu Q. Slicing, Stacking and Rolling: Fabrication of Nanostructured Collagen Constructs from Tendon Sections. *Adv Healthc Mater* 2013; **2**:817–21.
12. Alberti KA, Hopkins AM, Tang-Schomer MD *et al*. The behavior of neuronal cells on tendon-derived collagen sheets as potential substrates for nerve regeneration. *Biomaterials* 2014; **35**:3551–7.
13. Alberti K, Wang J, Xu Q. in vivo Peripheral Nerve Repair Using Tendon-derived Nerve Guidance Conduits. *Submitted*.
14. Alberti KA, Sun JY, Illeperuma W *et al*. Laminar Tendon Composites with Enhanced Mechanical Properties. *J Mater Sci* 2014; **50**:2616–25.
15. Harper E, Berger a, Katchalski E. The hydrolysis of poly (L-Prolyl-Glycyl-L-Prolyl) by bacterial collagenase. *Biopolymers* 1972; **11**:1607–12.
16. Stenzel K, Miyata T, Rubin A. Collagen as a biomaterial. *Annu Rev Biophys Bioeng* 1974; **3**:231–53.
17. Yannas IV, Burke JF, Huang C *et al*. Correlation of in vitro collagen degradation rate with in vivo measurements. *J Biomed Mater Res* 2004; **9**:623–8.
18. Sung HW, Hsu CS, Wang SP *et al*. Degradation potential of biological tissues fixed with various fixatives: an in vitro study. *J Biomed Mater Res* 1997; **35**:147–55.
19. Thompson DM, Buettner HM. Neurite outgrowth is directed by schwann cell alignment in the absence of other guidance cues. *Ann Biomed Eng* 2006; **34**:161–8.
20. Anderson JM, Shive MS. Biodegradation and biocompatibility of PLA and PLGA microspheres. *Adv Drug Deliv Rev* 2012; **64**:72–82.
21. Baker JL, Chandler ML, LeVier RR. Occurrence and activity of myofibroblasts in human capsular tissue surrounding mammary implants. *Plast Reconstr Surg* 1981; **68**:905–12.
22. Majd H, Scherer SS, Boo S *et al*. Novel micropatterns mechanically control fibrotic reactions at the surface of silicone implants. *Biomaterials* 2015; **54**:136–47.
23. Brown BN, Badylak SF. Extracellular matrix as an inductive scaffold for functional tissue reconstruction. *Transl Res* 2014; **163**:268–85.

24. Oliver RF, Barker H, Cooke A *et al*. Dermal collagen implants. *Biomaterials* 1982; **3**:38–40.
25. Anderson J, Rodriguez A, Change D. Foreign Body Reaction to Biomaterials. *Semin Immunol* 2008; **20**:86–100.
26. Floden EW, Malak SFF, Basil-Jones MM *et al*. Biophysical characterization of ovine forestomach extracellular matrix biomaterials. *J Biomed Mater Res - Part B Appl Biomater* 2011; **96 B**:67–75.
27. Valentin JE, Stewart-Akers AM, Gilbert TW *et al*. Macrophage participation in the degradation and remodeling of extracellular matrix scaffolds. *Tissue Eng Part A* 2009; **15**:1687–94.
28. Oliver R, Hulme M, Mudie A *et al*. Skin collagen allografts in the rat. *Nature* 1975; **258**:537–9.
29. Oliver R, Grant R, Cox R *et al*. Histological studies of subcutaneous and intraperitoneal implants of trypsin prepared dermal collagen allografts in the rat. *Clin Orthop Relat Res* 1976;**115**.
30. Oliver RF, Grant Ra, Kent CM. The fate of cutaneously and subcutaneously implanted trypsin purified dermal collagen in the pig. *Br J Exp Pathol* 1972; **53**:540–9.
31. Griffiths RW, Shakespeare PG. Human dermal collagen allografts: a three year histological study. *Br J Plast Surg* 1982; **35**:519–23.
32. Macleod TM, Williams G, Sanders R *et al*. Histological evaluation of Permacol as a subcutaneous implant over a 20-week period in the rat model. *Br J Plast Surg* 2005; **58**:518–32.
33. Eppley BL. Experimental assessment of the revascularization of acellular human dermis for soft-tissue augmentation. *Plast Reconstr Surg* 2001; **107**:757–62.
34. DeLustro F, Smith ST, Sundsmo J *et al*. Reaction to injectable collagen: results in animal models and clinical use. *Plast Reconstr Surg* 1987; **79**:581–94.
35. DeLustro F, Dasch J, Keefe J *et al*. Immune responses to allogeneic and xenogeneic implants of collagen and collagen derivatives. *Clin Orthop Relat Res* 1990; **260**:263–79.